Overlooked effects of wavefront reception with or without speed limit, from aberration to time measurement

Denis Michel

Overlooked effects of wavefront reception with or without speed limit, from aberration to time measurement

Denis Michel

Université de Rennes, Irset, Rennes, France. E-mail: denis.michel@live.fr

The measurement of durations, Doppler and aberration effects and cosmological redshift, are all perceptual phenomena, and as such require the use of reception rather than Lorentz-transformed coordinates. Perceived durations relate proper to proper durations while the famous time dilation of special relativity relates proper to improper durations. Taking this subtlety into account rehabilitates the controversial Poincaré ellipsoid whose polar equation is just the relativistic Doppler effect and which in no way questions the sphericity of light wavefronts in all frames. The transposition of this approach to the Galilean case whose transformed and received wavefronts are homothetic, reveals new aberration relations and the existence of a transverse Doppler effect very similar, in proportion to the respective wave velocities, to the relativistic one, thus forbidding in practice the test of his theory proposed by Einstein. The reasons for the long persistence of a classical angular Doppler formula divorced from wavefront reception are discussed, one of them ironically being the theory of special relativity.

Keywords:
Wavefront reception, transverse Doppler effect, aberration, relativity, time measurement.

1 Introduction

The viewing of a distant scene transmitted by light at the frequency of one frame per wave crest, would appear accelerated if the periods were shortened and slowed if the periods were lengthened. The time marked by a clock viewed on this film would appear modified in the same way compared to our local clock. On the other hand, special relativity says that a clock in uniform motion is slowed down by a Lorentz factor (γ) with respect to ours. In fact these two phenomena are not equivalent because the measured time distortions do not correspond to the orientation-independent time dilation of special relativity which is not directly perceived but calculated. Clarifying this point removes misunderstandings, resolves long-standing debates and rehabilitates Poincaré's ellipsoidal wavefront theory. Transposing the electromagnetic wavefront approach to its Galilean counterpart is even more instructive and allows to improve the current aberration and Doppler rules.

2 To change the perception of time by changing the waves

2.1 The prediction of Lemaître

Before the celebrated publication of Hubble, Lemaître had shown that wavelengths should follow expansion [1]. For an interval of universe

$$ds^2 = dt^2 - a(t)^2 d\sigma^2 \tag{1}$$

where $d\sigma$ Is the element length of a space of radius equal to 1, the equation of a light beam is

$$\sigma_2 - \sigma_1 = \int_{t_1}^{t_2} \frac{dt}{a} \tag{2}$$

where σ_1 and σ_2 are the coordinates of a source and an observer. A beam emitted later at $t_1 + \delta t_1$ and arriving at $t_2 + \delta t_2$ undergoes a shift such that

$$\frac{\delta t_2}{a_2} - \frac{\delta t_1}{a_1} = 0 \tag{3}$$

giving

$$z = \frac{\delta t_2}{\delta t_1} - 1 = \frac{a_2}{a_1} - 1 \tag{4}$$

where δt_1 and δt_2 can be considered as the periods at emission and reception respectively [1]. If a procession of regularly spaced walkers crosses a stretching rubber band, their spacing on arrival will obviously be stretched in the same ratio as the rubber band. The same reasoning applies to a series of wave crests. In his article, Lemaître called this effect a Doppler effect [1]. This term is acceptable if it is broadly defined as a wave distortion, but this is not the classical Doppler effect related to the speed of the source which will be addressed later. The ratio of the received wavelength to the emitted wavelength simply follows the increase in the distance D between the source and the receiver that occured during the light's journey:

$$\frac{T^{\text{app}}}{T} = \frac{D_{\text{reception}}}{D_{\text{emission}}} \tag{5}$$

This generalized increase in wavelength, known as the cosmological redshift, is evaluated by comparing standard values such as atomic rays which are all identical as long as they are measured in their inertial rest frames. This redshift is entirely a phenomenon of wave distortion, which holds even if the sources and the receivers belong to the same inertial frame.

2.2 The observation: the slowing of time by stretching waves

A proof of the direct relation between the electromagnetic wave stretching and the durations comes from an astronomical observation, not originally intended for this purpose, made in the context of the expansion of the universe thanks to the type Ia supernovae (SNIa). SNIa are stellar explosions that are extremely luminous for a certain stereotypical duration, and which can be seen from very far away. The light from some very distant and therefore very old SNIa took a long time to reach us, and as space expanded during the light's journey, it stretched its wavelengths. In this context, a striking phenomenon was noticed: The duration of the brightness of SNIa depends on their distance, in exact proportion to their redshift, i.e. to the lengthening of the period.

$$\frac{\Delta t^{\text{app}}}{\Delta t} = \frac{T^{\text{app}}}{T} \tag{6}$$

For example, a distant SNIa with a redshift of $T^{\text{app}}/T = 1.5$, has a brightness duration that is exactly 1.5 times longer [2]. This observation shows that the simple fact of decreasing the frequency of the waves, increases the apparent durations. If we consider the question carefully, there is no magic here: the same scene viewed at 30 frames per second when the wavelengths are not stretched ($T^{\text{app}}/T_0 = 1$) is viewed at 20 frames per second when the wavelengths are stretched by $T^{\text{app}}/T_0 = 1.5$, and therefore the viewing time will necessarily be longer to receive all the frames of the scene.

2.3 Wave reception is a physical process

The perception of compressed or expanded waves is not a simple optical illusion because the physical effects are real. A clear example is provided by the technique of atomic cooling. An atom can be immobilized by illuminating it from all sides with streams of light. As the atom moves in a given direction, the Doppler effect causes the light frequency, and therefore the light energy, to increase in front of it and decrease behind it, bringing the atom back to its original position [3].

3 Limit speed and causality

3.1 The limit speed of light

Physical laws are such that apparent inconcistencies are eliminated. A typical example is the speed limit of light, which prevents us from witnessing incongruous scenes and having to reconstruct them later. We have never seen a soap bubble appear spontaneously from a cloud of droplets and then disappear into the tube of an experimenter who sucks it in. However, this is the vision we might have in the absence of limit velocity as shown in Fig.1. As shown by the arrows at the top of the diagram, as the car moves forward, the images of the bubble arrive at a greater distance from the observer O_B at the back of the car, and at a smaller distance from the observer O_F at the front of the car. Hypothetically, if the speed of the car exceeded the speed of light ($v > c$), O_F could witness a reverse scene, the bursting of the bubble before its birth. Such a perception, which violates the principle of causality, is prevented by the unsurpassable speed of light. At worst, in the asymptotic case of a car traveling at nearly c, the birth and bursting of the bubble would appear to be simultaneous, and its lifetime would tend toward zero, but would never be negative. By comparison, if there were no speed limit, we could see the consequences before the causes.

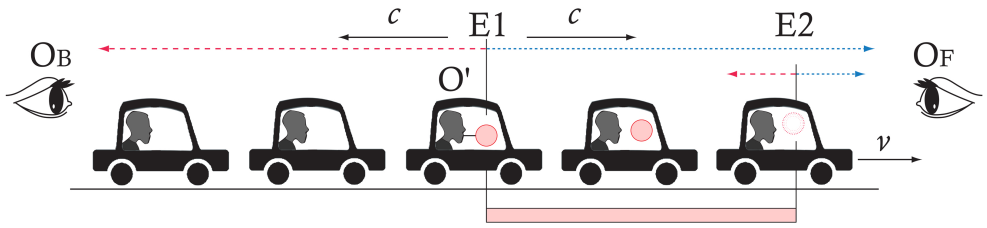

Figure 1. Events of birth ($E1$) and disappearance ($E2$) of a soap bubble in a vehicle moving at constant speed v with respect to observers, one located at the back (O_B) and the other at the front (O_F) of the vehicle. The images of the formation and the bursting of the bubble reach the observers at the speed of light c.

3.2 Causality break in the absence of speed limit

In the soap bubble experiment of Fig.1, the vehicle can never reach the speed limit c of the wave carrying its image. As a consequence, the causal order of the events is necessarily respected visually. We will always see bubbles burst after they form, regardless of their relative speed with respect to any observer. This sequence of events respects causality and is consistent with the statistical arrow of time. But what would have happened if there had been no speed limit? Let us imagine that the duration of the bubble is no longer measured visually but acoustically, assuming that tic and tac sounds are emitted when the bubble is born and when it bursts, and that the vehicle is a fast aircraft that exceeds the speed of sound. If it were technically possible to listen to the sounds in the cockpit of the plane that broke the sound barrier and assuming the existence of sound intensity corrections, we would hear the bubble bursting before it appeared, as if on a soundtrack played backwards. We would also hear the pilot (un)swallow his coffee before it was (un)poured into his cup. In the absence of a speed limit, the wavefronts can arrive at the receptor as separate bubbles that are reversed in time, as shown by Christian Doppler in 1847 in his diagram of the cone of successive wavefronts emitted by a supersonic source [4] (right panel in Fig.2 for $\beta > 1$).

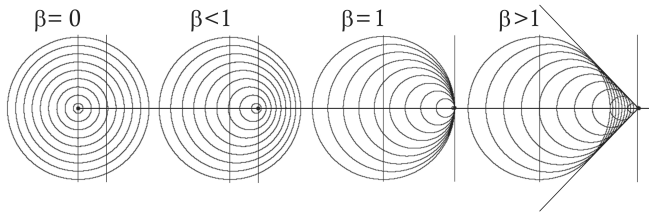

Figure 2. Time reversal between sending and receiving for $\beta = 1$, the sound barrier for the sound wave. For $\beta > 1$, the most recently emitted wavefronts are received first.

4 Orientation-dependent perception of durations

The association between the redshift and the duration [2] illustrates the connection between perceived time and period distortion. Applying this principle to the kinetic Doppler effect, the occupants of a vehicle coming toward us should move rapidly, and then suddenly slow down as it moves away from us. As shown below, this is indeed what the theory of special relativity predicts. To illustrate this, let us calculate the apparent lifetime of the soap bubble inside the moving vehicle.

4.1 Orientation-dependent relativistic duration measurement

The basic tools of special relativity allow to demonstrate the nature of the perceived time. In the frame of reference R of the eyes in Fig.1, let us consider the point of view of O_B who sees the car O' moving away from him. In the reference frame of the car R', a soap bubble is temporarily formed. The clocks of O_B and O' are synchronized and coincide at $t = t'$ when they cross each other. Let us consider the spacetime coordinates of the events: formation of the bubble ($E1$) and the reception of this image by O_B (E_R). The image of the appearance of the bubble is emitted by the car O' at t'_{E1} and is received by O_B at a date which he notes t_R at the location $x_R = 0$. The corresponding coordinates in R' are given by Lorentz transformations:

$$x'_R = \gamma\left(x_R - \beta c t_R\right) = -\gamma\beta c t_R \tag{7a}$$

$$t'_R = \gamma\left(t_R - \frac{\beta x_R}{c}\right) = \gamma t_R \tag{7b}$$

The date t'_E of the appearance of the bubble in R' can be deduced from the distance traveled by the light ray in R'. The speed of the light ray c is given by the ratio

$$c = \frac{x'_E - x'_R}{t'_R - t'_E} = \frac{0 - (-\gamma\beta c t_R)}{\gamma t_R - t'_E} \tag{8a}$$

from which

$$t'_E = \gamma t_R(1-\beta) = t_R\sqrt{\frac{1-\beta}{1+\beta}} \tag{8b}$$

This equation establishes the relation between the date of emission by O' of the image of the event $E1$, and the date of reception t_R of its image by O_B. The same reasoning is valid for the events of birth and bursting of the bubble, which gives a life interval of the bubble

$$\Delta t_R = \Delta t'_E\sqrt{\frac{1+\beta}{1-\beta}} \tag{9}$$

We simply rediscover the relativistic Doppler effect here, because the events $E1$ and $E2$ can just as well be the emissions of two successive wave crests. The reception events take place at the same location in the reference frame R, so the time interval between them Δt_R is a proper time for O_B. The emission events take place at the same location in the reference frame R', so the time interval between them $\Delta t'_E$ is a proper duration for O'. The proper lifetime of the bubble for O', appears extended in the time of O_B, in a ratio different from the γ factor of the time dilation of special relativity. The latter is not directly perceived but can be calculated mathematically as follows. Once the coordinates in R' are obtained ($x'_{E1} = 0$ and $t'_{E1} = \gamma t_R(1-\beta)$), we can determine them in R by

applying the Lorentz transformations in the other direction

$$x_{E1} = \gamma\left(x'_{E1} + \beta c t'_{E1}\right) = \gamma\beta c t_R \sqrt{\frac{1-\beta}{1+\beta}} = \frac{\beta c t_R}{1+\beta} \quad (10a)$$

$$t_{E1} = \gamma\left(t'_{E1} + \frac{\beta x'_{E1}}{c}\right) = \gamma^2 t_R(1-\beta) = \frac{t_R}{1+\beta} \quad (10b)$$

By substituting in this last equation the value of t_R as a function of t'_{E1},

$$t_{R1} = t_{E1}(1+\beta) = t'_{E1}\sqrt{\frac{1+\beta}{1-\beta}} \quad (11a)$$

The relation between t_{E1} to t'_{E1} is obtained

$$t_{E1} = \frac{t'_{E1}}{\sqrt{1-\beta^2}} \quad (11b)$$

and as the next event of bursting of the bubble $E2$, follows the same rule,

$$\Delta t_E = \Delta t'_E\ \gamma \quad (11c)$$

The time dilation of special relativity is verified, but Δt_E cannot be timed by O_B because it is no longer a proper duration, since $E1$ and $E2$ do not occur at the same place in R. The time dilation of special relativity puts in relation a proper duration and an improper duration, which cannot be measured directly.

Similar calculations can be made for the reception of images by O_F, still in R but at the front of the vehicle. The suffix R now refers to the reception of images by O_F while keeping the same orientation of the x axis, we have

$$x'_R = \gamma\left(x_R + \beta c t_R\right) = \gamma\beta c t_R \quad (12a)$$

$$t'_R = \gamma\left(t_R + \frac{\beta x_R}{c}\right) = \gamma t_R \quad (12b)$$

The light ray carrying to O_F the image of the appearance of the bubble has speed

$$c = \frac{x'_R - x'_{E1}}{t'_R - t'_{E1}} = \frac{-\gamma\beta c t_R}{\gamma t_R - t'_{E1}} \quad (13a)$$

from which

$$t'_{E1} = \gamma t_R(1+\beta) = t_R\sqrt{\frac{1+\beta}{1-\beta}} \quad (13b)$$

Repeating the same process for the image of the bubble bursting, the observer O_F measures a shorter life of the bubble with his stopwatch.

$$\Delta t_R = \Delta t'_E\sqrt{\frac{1-\beta}{1+\beta}} \quad (14)$$

But again, this does not change the relativistic time dilation, because for O_F,

$$x_{E1} = \gamma\left(x'_{E1} + \beta c t'_{E1}\right) = \gamma\beta c t_R \sqrt{\frac{1+\beta}{1-\beta}} = \frac{\beta c t_R}{1-\beta} \quad (15a)$$

$$t_{E1} = \gamma\left(t'_{E1} + \frac{\beta x'_{E1}}{c}\right) = \gamma^2 t_R(1+\beta) = \frac{t_R}{1-\beta} \quad (15b)$$

and thus always

$$t_{E1} = \frac{t_R}{1-\beta} = \frac{1}{1-\beta}\ t'_{E1}\ \sqrt{\frac{1-\beta}{1+\beta}} = t'_{E1}\gamma \quad (16)$$

The time dilation actually measured by each point of a rest frame depends not only on the velocity modulus v of the moving reference frame, but also on the velocity vector $\vec{v}$. It will therefore be interesting to average these measurements for all possible orientations (see section 7).

4.2 Orientation-dependent "Galilean lifetime" measurement

Electromagnetic time results from the speed limit of light combining time and space. But let us repeat the previous calculation of the lifetime of the soap bubble using only a Galilean wave emitted by the soap bubble, keeping the notation but replacing the Lorentz transformations by the Galilean transformations. The corresponding coordinates in R' are given by:

$$x'_R = x_R - \beta c t_R = -\beta c t_R \quad (17a)$$

$$t'_R = t_R \quad (17b)$$

The date t'_E of the appearance of the bubble in R' can be deduced from the distance traveled by the Galilean ray at R', whose speed c is given by

$$c = \frac{x'_E - x'_R}{t'_R - t'_E} = \frac{0 - (-\beta c t_R)}{t_R - t'_E} \quad (18a)$$

giving

$$t'_E = t_R\ (1-\beta) \quad (18b)$$

The "Galilean lifetime" of the bubble is thus increased

$$\Delta t_{RB} = \frac{\Delta t'_E}{1-\beta} \quad (19a)$$

and without redoing the whole calculation, we understand that for the observer O_F

$$\Delta t_{RF} = \frac{\Delta t'_E}{1+\beta} \quad (19b)$$

As expected, we find the classical longitudinal Doppler effect.

5 Doppler effects calculated from the perceived wavefront surfaces

According to the dictionary, time is perceived as the sequence of events. The density of the stream of received images will naturally affect the tempo. This density is modified by the speed of the source relative to the receiver through the Doppler effect which has been introduced in an academic way above in the section 4, but this extensive method was limited to the elementary collinear case. The very general non-academic approach used below will give the results in all directions at once, both for the Doppler effect and for the aberration relations. Moreover, it allows to revise previously established Galilean relations. Concerning the relativistic aspect, this approach restores all its importance and validity to the Poincaré ellipsoid that remains subject to persistent debate. In order too better understand Poincaré's argument, let us establish its basis.

5.1 The coordinates of the light front describe a sphere in all reference frames

Since light propagates at the same speed in all directions, its wavefront is necessarily spherical. Moreover, since the speed of light is the same in all reference frames, a sphere of a light wave in one reference frame S' must also be a sphere in the reference frame S. This is indeed what the Lorentz transformations ensure. The sphere

$$x'^2 + y'^2 + z'^2 = (ct')^2 \tag{20a}$$

transformed using

$$x' = \frac{x + \beta ct}{\sqrt{1-\beta^2}},\ y' = y,\ z' = z \text{ and } t' = \frac{t + \frac{\beta x}{c}}{\sqrt{1-\beta^2}}$$

becomes

$$\frac{(x+\beta ct)^2}{1-\beta^2} + y^2 + z^2 = \frac{(ct+\beta x)^2}{1-\beta^2} \tag{20b}$$

which simplifies into

$$x^2 + y^2 + z^2 = (ct)^2 \tag{20c}$$

There is no discussion about this result which highlights the power of Lorentz transformations and no point in trying to oppose the sphere attributed to Einstein and the ellipse attributed to Poincaré [5], since both authors were aware that a Lorentz-transformed light sphere is a light sphere, received as an ellipsoid by an observer in relative motion [6, 7]. It happens that Doppler, aberration and measured time are reception effects and that confusing the reception coordinates with those designed to ensure Lorentz invariance, would misleadingly suggest a violation of the Lorentz invariant as for example in [8].

5.2 Contraction of lengths and of length-measuring instruments

The contraction of lengths in the direction of displacement continues to intrigue the general public because it has never been detected; but is it detectable in practice? Measuring an object means using an instrument in the reference frame of that object. So if the object moves along x, the x dimension of the measuring instrument will be shortened in the same ratio, making any detection impossible. But as Poincaré pointed out, if one does not use a material object as a measuring instrument, but an electromagnetic wave path (which is not subject to length shortening), then the wave path should appear stretched by comparison along x and take the form of an ellipsoid [5, 6, 7, 8, 9, 10] with a transverse/longitudinal axis ratio of $\sqrt{1-\beta^2}$.

5.3 Equations of the spheres of the mobile frame

5.3.1 The material sphere

From the mobile coordinate system, the surface of a material sphere of radius 1 has the equation

$$x'^2 + y'^2 + z'^2 = 1 \tag{21}$$

But from the fixed coordinate system, the sphere seen in its entirety would appear flattened in the x direction of motion. According to the Lorentz transformation for the x axis at $t = 0$,

$$\left(\frac{x}{\sqrt{1-\beta^2}}\right)^2 + y^2 + z^2 = 1 \tag{22}$$

as defined by Einstein in chapter 4 of [6]. It can be converted in polar coordinates using $x = \rho\sin\theta\cos\varphi$, $y = \rho\sin\theta\sin\varphi$ and $z = \rho\cos\theta$, for $R = 1$,

$$\rho = \sqrt{\frac{1-\beta^2}{1-\beta^2\left(1-\sin^2\theta\cos^2\varphi\right)}} \tag{23}$$

whose shape is represented in Fig.3A. It reduces in the two spatial dimensions $x = \rho\cos\theta$ and $y = \rho\sin\theta$ into the ellipse flattened along the x direction:

$$\rho = \sqrt{\frac{1-\beta^2}{1-\beta^2\sin^2\theta}} \tag{24}$$

5.3.2 The light wavefront

The speed of light is constant in all frames and always give 45° lines in all Minkowski diagrams regardless of the chosen point of view at rest. The time set above to zero is now set to one period conceived as the interval between two successive images. Inserting the period given by the

fourth transformation into the first transformation (of x') gives

$$x' = x\sqrt{1-\beta^2} + \beta c T' \tag{25}$$

Using $c = 1$ as Poincaré did, the surface of a single-period wavefront is the ellipsoid of equation

$$(x\sqrt{1-\beta^2} + \beta)^2 + y^2 + z^2 = 1 \tag{26}$$

whose conversion in polar coordinates yields the remarkably elegant equation

$$\rho = \frac{\sqrt{1-\beta^2}}{1 + \beta \sin\theta \cos\varphi} \tag{27}$$

plotted in Fig.3B.

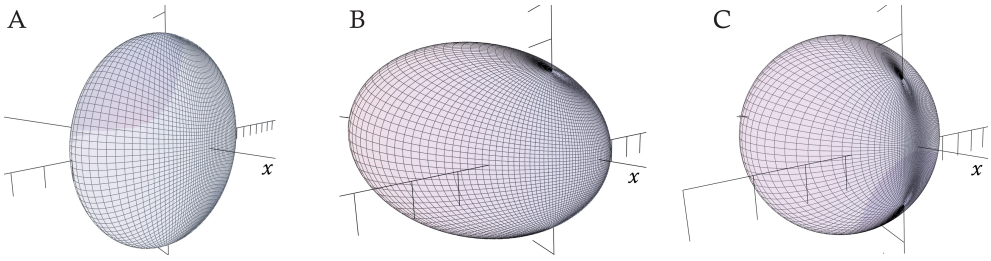

Figure 2. Perspective view of the shapes of (**A**) the material sphere drawn to Eq.(23), (**B**) the received relativistic wavefront surface drawn to (27) and (**C**) the Galilean wavefront drawn to Eq. Eq.(30), for $\beta = 0.9$. In the wavefront panels B and C, the source is located at the intersection of the axes.

It reduces in 2D polar coordinates to an ellipse. The radius ρ is changed for the receiver from $\rho_0 = 1$ in the same ratio as the apparent wavelength.

$$\frac{\rho}{\rho_0} = \frac{\lambda^{\text{mov}}}{\lambda} = \frac{\sqrt{1-\beta^2}}{1 + \beta\cos\theta} \tag{28}$$

This polar equation gives the complete collection of focal rays from the source to the wavefront surface for one period, so this is also the equation for the Doppler effect. We naturally recover the rays collinear to the path of the source in front of and behind it, which were laboriously determined in section 4, but also all the other rays.

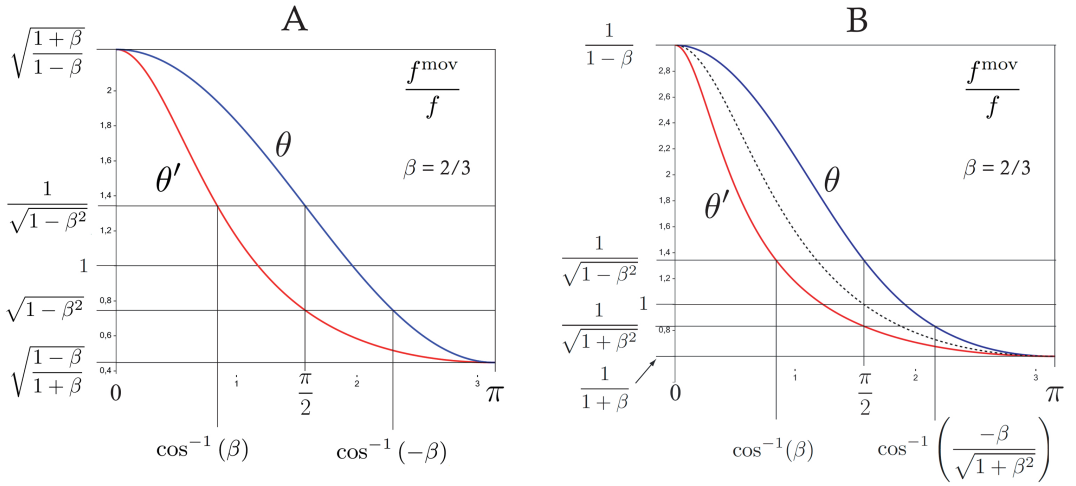

Figure 4. Doppler effects as functions of the angles θ and θ'. Since the true determinants of energies and colors are frequencies, Doppler effects are described using frequency ratios (**A**) Relativistic Doppler effect deduced from the perceived ellipsoidal wavefront. (**B**) Galilean Doppler effect deduced from the perceived spherical wavefront. The dotted black curve corresponds to the so-called classical Doppler effect, shown for comparison.

5.3.3 The Galilean wavefront

Of course the Lorentz transformations based on the speed limit apply in all circumstances, but they can be approximated by Galilean transformations when the electromagnetic β is close to zero, as for example for the sound wave whose speed has no common measure with that of light. However, the same letter β is kept here to express the Doppler formulas for ease of comparison. The Galilean transformations are simple: $x' = x + vt$, $y' = y$, $z' = z$ and $t' = t$. Hence, the surface of the Galilean wavefront emitted from a source moving of velocity v in direction x,

is a sphere of the Cartesian equation

$$(x+vt)^2+y^2+z^2=(ct)^2 \tag{29a}$$

Keeping the notation $\beta=v/c$ where c is no longer a speed limit, for a time corresponding to a single period unit,

$$(x+\beta)^2+y^2+z^2=1 \tag{29b}$$

The wavelengths are directly obtained by converting this Cartesian equation in polar equation.

$$\rho=\sqrt{1-\beta^2\left(1-\sin^2\theta\cos^2\varphi\right)}-\beta\sin\theta\cos\varphi \tag{30}$$

shown in Fig.3C and which reduces in 2D in the Galilean circle

$$\frac{\rho}{\rho_0}=\frac{\lambda^{\text{mov}}}{\lambda}=\sqrt{1-\beta^2\sin^2\theta}-\beta\cos\theta \tag{31}$$

whose off-centre aspect can also be understood as a change of the wave vector for the receiver [11, 12]. This Doppler effect expressed with frequencies is represented on Fig.4B. The notable points of these curves are listed in the tables 1 and 2 of appendix B. Note in these tables that for $\theta=\pi/2$ (yellow lines in the tables), the results for the relativistic and Galilean Doppler effects are identical. The Doppler effects found in this way are functions of the angle θ between the trajectory of the source and the source-receiver line exactly when the Doppler effect is received. But because of the travel time of the wave, the source is no longer in the position it was when it emitted both its image and the wave crests involved in the measured Doppler effect. The difference between this angle noted θ' and θ defines the phenomenon of aberration, long understood by Bradley in astronomy. Although Bradley's discovery largely predates the theory of relativity, today the relativistic aberration rules established by Einstein are well known but strangely their Galilean counterparts are generally ignored, which may explain the problems existing with the classical Doppler formula.

5.3.4 Derivation of aberration and Doppler formulas from wavefront surfaces

• Relativistic aberration

The relativistic ellipsoid is wider on the x axis by $1/\sqrt{1-\beta^2}$, which renders the geometric comparison with the sphere difficult. To make their diameters coincide on x while preserving the proportions of the ellipse, let us just contract the radius orthogonal to the trajectory, from 1 to $\sqrt{1-\beta^2}$. For a source moving from left to right, the Cartesian equation of this simplified ellipse is

$$(x+\beta)^2+\frac{y^2}{1-\beta^2}=1 \tag{32}$$

whose polar equation obtained using $x=\rho\cos\theta$ and $y=\rho\sin\theta$

$$\rho=\frac{1-\beta^2}{1+\beta\cos\theta} \tag{33}$$

allows us to easily obtain the aberration relations because as it is not directional, the relativistic dilation transforms the ellipse in a homothetic way without changing its characteristics and angles. Since the intersection of the focal radius ρ and the perimeter of the ellipse does not correspond to a point tangential to the radius emanating from the center of the ellipse, let us consider the fixed frame of reference of this center from which the wave front propagated with spherical symmetry. We have

$$\cos\theta'=\frac{\beta+\rho\cos\theta}{R} \tag{34a}$$

where R is the large radius without flattening fixed at 1. Using the value of ρ given in Eq.(33), this equation becomes

$$\cos\theta'=\frac{\cos\theta+\beta}{1+\beta\cos\theta} \tag{34b}$$

whose reciprocal form is as elegant.

$$\cos\theta=\frac{\cos\theta'-\beta}{1-\beta\cos\theta'} \tag{34c}$$

These aberration relations can then be expressed in other ways

$$\sin\theta'=\sin\left(\cos^{-1}\left(\frac{\cos\theta+\beta}{1+\beta\cos\theta}\right)\right)=\frac{\sqrt{1-\beta^2}\sin\theta}{1+\beta\cos\theta}$$

and

$$\tan\theta'=\frac{\sin\theta'}{\cos\theta'}=\frac{\sin\theta\sqrt{1-\beta^2}}{\beta+\cos\theta} \tag{35}$$

• Two relativistic Doppler equations

Using the aberration relations, the Doppler effect can be written in two ways

$$\frac{f^{\text{mov}}_{(\theta)}}{f}=\frac{1+\beta\cos\theta}{\sqrt{1-\beta^2}} \tag{36a}$$

$$\frac{f^{\text{mov}}_{(\theta')}}{f}=\frac{\sqrt{1-\beta^2}}{1-\beta\cos\theta'} \tag{36b}$$

A more standard demonstration of these formulas is described in [6] and further detailed in [13].

• Galilean aberration

In the Galilean case,

$$\cos\theta'=\frac{\beta+\rho\cos\theta}{R} \tag{37a}$$

For $R=1$ and expressing ρ as function of the angle θ (Eq.(31))

$$\cos\theta'=\cos\theta\sqrt{1-\beta^2\sin^2\theta}+\beta\sin^2\theta \tag{37b}$$

and conversely

$$\cos\theta = \frac{\cos\theta' - \beta}{\sqrt{1+\beta^2-2\beta\cos\theta'}} \tag{37c}$$

giving for the tangent

$$\begin{aligned}\tan\theta' &= \frac{\rho\sin\theta}{\beta+\rho\cos\theta} \\ &= \frac{\sin\theta\left(\sqrt{1-\beta^2\sin^2\theta}-\beta\cos\theta\right)}{\cos\theta\sqrt{1-\beta^2\sin^2\theta}+\beta\sin^2\theta}\end{aligned} \tag{37d}$$

These new aberration relations were introduced in [9].

• Two Galilean Doppler equations

As for the relativistic case, two Galilean Doppler formulas related through these reciprocal aberration relations, can be established depending on the angle considered. The Doppler formula as a function of θ

$$\frac{f^{\text{mov}}_{(\theta)}}{f} = \frac{1}{\sqrt{1-\beta^2\sin^2\theta}-\beta\cos\theta} \tag{38}$$

was found above as the focal radius from the actual position of the source to the wavefront which holds regardless of the distance of the receptor because at that position the successive wavefronts are equidistant from the source. But the successive intervals between the point of emission and the point of reception are, of course, no longer the same, so that the Doppler formula as a function of θ' must be derived differently, for example by applying the aberration relations to the Doppler function of θ.

$$\frac{f^{\text{mov}}_{(\theta')}}{f} = \frac{1}{\sqrt{1+\beta^2-2\beta\cos\theta'}} \tag{39}$$

This function of θ' can be also be confirmed geometrically using the cosine law. Incidentally, Eq.(31) can also be found in this way but it does not hold for the the optical Doppler effect as assumed in [14] because spherical geometry cannot apply in this case. For the angle θ', let us imagine, as shown in Fig.5, that a source S located at an unspecified distance from a receiver $c\Delta t_1$, emits a signal and that at the same time as this signal is received, it emits a second signal. This situation makes it possible to compare the durations for the source with the durations of the source perceived by the receiver. In fact, by fixing the time of origin $t = 0$ when the source is at the position S_1 (Fig.5), then the duration that elapses between the two signals at the source is Δt_1. Besides, for the receiver and in Galilean coordinates, the first signal is received at time $t_a = \Delta t_1$ and the second signal is received at time $t_b = \Delta t_1 + \Delta t_2$, which gives a duration between the two reception events of $t_b - t_a = \Delta t_2$.

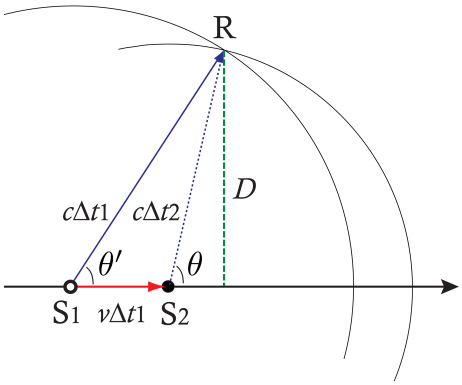

Figure 5. Two successive pulses are sent to the receptor, with the second pulse being sent exactly when the first is received.

So the ratio between the perceived and local durations of the source is simply given by the ratio $\Delta t_2/\Delta t_1$. This is the Doppler effect, whether this duration is a wave period or not, as was shown previously for the lifetime of the soap bubble. All that remains is to find this ratio geometrically. During the first signal's journey, the source will have travelled $v\Delta t_1$. So on the one hand we have

$$D = c\Delta t_1 \ \sin\theta' = c\Delta t_2 \ \sin\theta \tag{40a}$$

and on the other hand, the cosine law gives

$$(c\Delta t_1)^2 + (v\Delta t_1)^2 - 2vc\Delta t_1^2\cos\theta' = (c\Delta t_2)^2 \tag{40b}$$

The combination of these two equations gives

$$\begin{aligned}\sin\theta &= \frac{c\Delta t_1\sin\theta'}{\sqrt{(c\Delta t_1)^2+(v\Delta t_1)^2-2vc\Delta t_1^2\cos\theta'}} \\ &= \frac{\sin\theta'}{\sqrt{1+\beta^2-2\beta\cos\theta'}}\end{aligned} \tag{40c}$$

as calculated reciprocally by Compton for a ray passing through a moving sphere [15]. Hence, the ratio of wavelengths is

$$\frac{c\Delta t_2}{c\Delta t_1} = \frac{\sin\theta'}{\sin\theta} = \sqrt{1+\beta^2-2\beta\cos\theta'} \tag{40d}$$

or

$$\frac{\Delta t_1}{\Delta t_2} = \frac{1}{\sqrt{1+\beta^2-2\beta\cos\theta'}} \tag{40e}$$

Again, this result which is identical to Eq.(39), is valid for any kind of duration. A Doppler effect basically relates a proper duration to a perceived duration, in both the relativistic and in the classical case, whether that duration is the lifetime of a soap bubble, as calculated in section 4, or the period of a wave. Introducing considerations such as fractions of a period of a wave would be unnecessarily disturbing. In fact, to the question what happens for a wave whose period is not exactly Δt_1, we can answer that in principle it is always possible to perform the experiment with the wave whose period is Δt_1. The number of Doppler formulas is not infinite, there is not one for every wavelength and for every source-observer distance. Furthermore, for a wave, calculations made for durations

of the order of a period or a fraction of a period would be meaningless for determining a Doppler effect, because they would overestimate its precision. A Doppler effect is not applicable for less than one period and can only be defined for a series of successive wave crests, for which the question of the phase coincidence disappears. Expressing the Doppler effect as a function of a precise angle θ' is illusory since the series of wave crests that allows it to be characterised does not correspond to a single θ' but to a small range of θ'. In fact the instantaneous frequency is never well defined for a continuously changing angle. Even for a collinear Doppler effect of a cosinusoidal signal

$$X(t) = \cos(2\pi f_0 t) \tag{41}$$

the imprecision of the frequency is given by the Fourier transform of this wave function and depends on the duration of the measurement. f_0 is obtained precisely only for the infinite signal duration of Eq.(41) by Dirac peaks (top panel of Fig.6)

$$X(f) = \frac{1}{2}\left[\delta(f - f_0) + \delta(f + f_0)\right] \tag{42}$$

But for a finite duration Δt, the wave function is

$$X(t) = \mathrm{rect}(t/\Delta t) \cdot \cos(2\pi f_0 t) \tag{43}$$

whose Fourier transform involves the cardinal sine function

$$X(f) = \frac{1}{2}\left|\frac{\sin(\pi\Delta t\ (f - f_0))}{\pi(f - f_0)} + \frac{\sin(\pi\Delta t\ (f + f_0))}{\pi(f + f_0)}\right| \tag{44}$$

whose graph shows a spread of the frequency peak with respect to f_0 and the appearance of parasite frequencies. In the example of a 40 Hz wave chosen for Fig.6, a listening duration of a single period results in a frequency uncertainty ranging from 0 to 80 Hz (bottom panel of Fig.6). The formal treatment of a wave bubble corresponding to a single period gives the correct result, but its application is irrelevant in practice. For physically relevant finite signals and particularly for a continuously changing angular Doppler effect, the product of the minimal imprecision in the frequency and the duration is a constant ($\Delta t \cdot \Delta f = 2$) and the window Δt is all the shorter, theoretically zero, as the evolution of θ is fast.

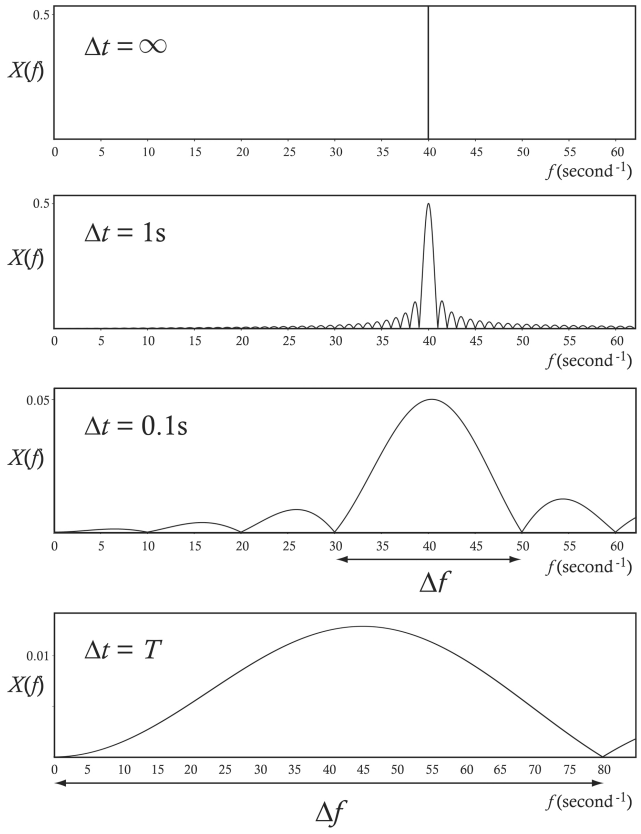

Figure 6. Increasing imprecision in frequency as the duration of the signal decreases. Example of a sound of 40 Hertz (40 cycles per second). An infinite (non-physical) duration of the sound allows the absolute focusing of its frequency (top panel). We observe a broadening of the frequency peak (Δf) and the appearance of parasite frequencies as the signal duration (Δt) is shortened.

6 How to explain the persistence of a questionable Galilean formula

The currently accepted Doppler formula, which describes the frequency change of a moving source perceived by a static observer is

$$\frac{f^{\mathrm{mov}}}{f} = \frac{1}{1 - \beta\cos\vartheta} \tag{45}$$

Its representation (dotted line in Fig.4B) gives an intermediate curve which does not allow to decide about the nature of the angle ϑ between the trajectory of the source and the direction of the receiver. Its main characteristic is to cancel (value of 1) for an angle of $\pi/2$, but in the absence of a clear development of the classical Doppler formula, it is difficult to point to any specific error in its demonstration. However, a number of arguments questioning its validity are listed below.

6.1 The success of the perceived wavefront approach

An argument, specific to the present study, is to ask why, while the wavefront approach is so effective in recovering all the correct relativistic formulas, it would not work for the Galilean case.

6.2 An orphan formula disconnected from aberration

The collinear Galilean Doppler equations are identical for the traditional and the new formulas. They are also confirmed by the rigorous approach to wave reception in the section 4.2. However, the intermediate angular values differ significantly, especially in two aspects: (i) the existence of a transverse Doppler effect for the new formulas but not for the old one, and (ii) two new formulas, depending on whether they are expressed in terms of θ or θ', against only one old formula, as if the aberration had been neglected in the classical approach. The origin of the angle ϑ of Eq.(45) is the source but in addition, it is necessary to specify whether the position of the source is to be taken into account when the wave is emitted or received. In the treatments of [16] or [17], it corresponds to θ' used here, so in the following parts we will rewrite the Galilean Doppler formula as

$$\frac{f^{\text{mov}}}{f} = \frac{1}{1-\beta\cos\theta'} \tag{46}$$

In an attempt to reconcile the usual (Eq.(46)) and new Eq.(39) formulas, (Eq.(46)) could be rewritten as a square root of a square.

$$\frac{f^{\text{mov}}}{f} = \frac{1}{\sqrt{1+\beta^2\cos^2\theta' - 2\beta\cos\theta'}} \tag{47}$$

But we see that Eq.(47) and Eq.(39) are still different and that in addition, one cannot invoke the approximation of a very small angle θ' (which would make $\cos^2\theta' \approx 1$) because of the alleged prediction that the Doppler effect must vanish ($f^{\text{mov}}/f = 1$) when $\theta' = \pi/2$ and $\cos\theta' = 0$. Moreover, while Einstein presented the relativistic Doppler formulas in pairs and in conjunction with two reciprocal aberration relations, in the rare demonstrations of the Galilean Doppler effect (subsequently called classical in reference to relativistic) available in the literature, one finds no trace of an expression as a function of two angles, nor in conjunction with Galilean aberration rules. The aberration and Doppler formulas should be obtainable together from the same approach. Interestingly, a recent manuscript [17] proposes to combine the old Doppler formula with the Galilean aberration rule of the new Doppler formula [9]. However, this combination of Doppler and aberration formulas obtained in different ways, respectively approximate and strictly geometrical, leads to unacceptable consequences such as a non-spherical asymmetric wavefront.

6.3 Dual detection of the Doppler effect and of the position

An acceptable example of Galilean wave is provided by the sound, in the case of a source moving in a stationary propagation medium and a receiver stationary with respect to that medium. When measuring the Doppler shift of sound, the tracking of the source can lead to ambiguities in the estimation of the transverse position. The light Doppler effect is, of course, measured by pointing the telescope at the source, but we know that this source has changed location while the light was traveling toward the telescope, so that its true position is invisible. In contrast for a Galilean wave, the information about the Doppler effect and on the location of the source are carried by different channels and can be recovered simultaneously.

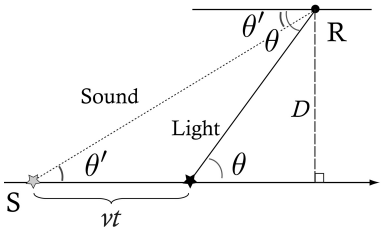

Figure 6. Since the speed of light can be considered as infinite compared to that of sound, the sound wave carrying the Doppler effect emitted by the source S under an angle θ' toward the receiver R, and the light carrying the image of the source, emitted under an angle θ toward the receiver, arrive together at the receiver. On the whole trajectory, D is the shortest distance between the source and the receiver.

As depicted in Fig.6, the Doppler effect of the sound is of course carried by the acoustic wave but the information about the position of the source is generally visual, i.e. carried by a light wave. This issue is concretely illustrated in the experimental application in Appendix A. If the source velocity is constant, both θ and θ' can be used, but if there is any doubt about the constancy of the velocity, then the use of θ' is preferable, but this requires the use of a highly directional microphone to identify the spatial origin of the sound. Note also that the Doppler effects of sound involve many more parameters concerning the relative motion between the three actors: source, receiver and medium, which will not be discussed here.

6.4 The classical Doppler formula could have been strenghened by the relativistic one

The traditional Doppler formula may have been consolidated by a resemblance to the relativistic Doppler effect. Indeed, the relativistic Doppler shift is often derived as if it were the classical phenomenon, but modified by the addition of a time dilation term as explained in certain textbooks [18, 19, 20, 21]. Thus, the classical formula of the Doppler effect Eq.(46) has probably been aided by the

advent of the relativistic Doppler effect, the form of which can suggest the confusing idea that it is simply the classical Doppler effect corrected by the relativistic dilation factor.

6.4.1 The puzzling idea that the classical Doppler effect is the "primary effect" of the relativistic one

According to approximate relativistic theories, the classical formula would be a primary Doppler effect of purely kinetic nature, which must be complemented by a so-called "secondary" effect of time dilation by the Lorentz factor (multiplication of the periods by $1/\sqrt{1-\beta^2}$) to obtain the relativistic Doppler effect. In fact, kinetic and temporal effects cannot be dissociated in relativity and the Lorentz factor itself includes the change in kinetic energy. Nevertheless, this questionable principle has been accepted because it seems to work. The multiplication by $\sqrt{1-\beta^2}$ of Eq.(46) does indeed give Eq.(36b), which is Einstein's relativistic Doppler formula where θ' is the reception angle. This unfortunate identity has logically reinforced the presumed validity of Eq.(46) as the classical Doppler effect formula for generations of researchers and teachers. The consensus created in the scientific community by this apparent proof probably inhibited naive questions such as, for instance, if the only difference between the classical and relativistic Doppler effects is the dilation of the periods for the latter, then why should the classical and relativistic aberration rules be different? In fact, the generalized correction by the dilation factor has a homothetic effect, which by itself cannot change the angles.

6.4.2 Additional confusion caused by an inappropriate wave averaging mode

The puzzling concept of the secondary Doppler effect, which is supposed to be specific to relativity and which probably gives credit to the current classical Doppler effect, has itself been consolidated by the inappropriate use of the arithmetic mean for averaging Doppler effects. In the articles validating the relativistic Doppler effect, longitudinal [22] and transverse [23], it is explained that the relativistic Doppler effect, unlike the classical one, includes a secondary transverse effect. Ives and Stilwell simultaneously measured the longitudinal wavelengths of approach (λ_a) and recession (λ_r), with and against the motion of the particles. They then compared the wavelength shifts to their so-called "center of gravity" which is conceived as an arithmetic mean [23]. Knowing the relativistic longitudinal effects to be demonstrated, they calculated

$$\begin{aligned}\lambda_{\text{mean}} &= \frac{\lambda_a + \lambda_r}{2} \\ &= \frac{1}{2}\left(\lambda_0 \sqrt{\frac{1-\beta}{1+\beta}} + \lambda_0 \sqrt{\frac{1+\beta}{1-\beta}}\right) \\ &= \frac{\lambda_0}{\sqrt{1-\beta^2}} \sim \lambda_0 + \frac{\lambda_0}{2}\beta^2\end{aligned} \tag{48}$$

They concluded that $\lambda_{\text{mean}} \neq \lambda_0$ due to transverse Doppler shift

$$\frac{\Delta\lambda}{\lambda_0} = \frac{\lambda_{\text{mean}} - \lambda_0}{\lambda_0} \sim \frac{1}{2}\beta^2$$

This conclusion results from a misuse of the arithmetic mean. Perhaps judging the appearance of Eq.(48) satisfactory, these authors did not look at what is going on for the frequency f_{mean} which corresponds to this λ_{mean}. However, since the collinear Doppler effect during the approach for wavelengths corresponds to the Doppler effect during the recession for frequencies and vice versa, they would have found that the result is the same

$$f_{\text{mean}} = \frac{f_0}{\sqrt{1-\beta^2}} \tag{49}$$

But for any photon, the product: frequency × wavelength is a well known constant

$$f\lambda = c \tag{50}$$

and therefore the above approach is obviously wrong as we would have

$$f_{\text{mean}}\ \lambda_{\text{mean}} = \frac{\nu_0\ \lambda_0}{1-\beta^2} \neq c \tag{51}$$

In fact, the arithmetic mean used in [22, 23] is inappropriate for averaging Doppler effects because as explained in section 7, it cannot work for both frequencies and wavelengths.

6.4.3 The transverse effect supposedly specific of relativity

Finally, the acceptance of the classical Doppler effect by the scientific community may have been favored by the mistaken intuition that it should cancel ($f^{\text{mov}}/f = 1$) when the source is the closest. The absence of Doppler shift predicted by the currently accepted equation Eq.(46) seems very reasonable [24], but it is nevertheless incorrect, as a rigorous analysis of the spherical wavefront (Table 2 in Appendix B) shows. For a moving source and static receiver, the Galilean transverse effect obtained for a reception angle $\theta' = \pi/2$, is

$$\left(\frac{f^{\text{mov}}}{f}\right)_{\text{transverse}} = \frac{1}{\sqrt{1+\beta^2}} \tag{52}$$

When this effect is received, the source is at the distance βD from the nearest point (Table 2). By comparison,

the famous relativistic transverse effect, which Einstein envisioned as a possible confirmation of special relativity theory [25], is

$$\left(\frac{f^{\text{mov}}}{f}\right)_{\text{transverse}} = \sqrt{1-\beta^2} \tag{53}$$

These effects are both $1-\frac{\beta^2}{2}+\mathcal{O}(\beta^4)$ and differ only by $\beta^4/4$, making the discrimination proposed by Einstein technically very delicate.

7 Mean Doppler effects

7.1 The appropriate mean for averaging frequencies

Mathematically, there are several modes of averaging that apply differently to the specific situations. These different types of averaging include, when applied to two Doppler effects,

- The arithmetic mean: $\frac{1}{2}\left(\frac{f_1^{\text{mov}}}{f}+\frac{f_2^{\text{mov}}}{f}\right)$
- The geometric mean: $\left(\frac{f_1^{\text{mov}}}{f}\frac{f_2^{\text{mov}}}{f}\right)^{\frac{1}{2}}$
- The harmonic mean: $\frac{2f}{f_1^{\text{mov}}+f_2^{\text{mov}}}$

The appropriate one is necessarily the geometric mean, because it is the only one that holds for both periods and frequencies, such that

$$\langle f_1, f_2\rangle = \frac{1}{\langle T_1, T_2\rangle} \tag{54}$$

As a matter of fact, the use of geometric averages for wavelengths has already been empirically applied and, in particular, satisfies the rule of color reflectance fusion.

7.2 Mean relativistic Doppler effect

The product involved in the geometric mean for all angles θ around the source using Eq.(36b) can be transformed into a sum by going through the logarithms. Expressed in periods

$$\begin{aligned}\left\langle\frac{T^{\text{mov}}}{T}\right\rangle &= \left(\prod_{\theta=0}^{\pi}\frac{T_{(\theta)}^{\text{mov}}}{T}\right)^{\frac{1}{\pi}}\\ &= \exp\left[\frac{1}{\pi}\int_{\theta=0}^{\pi}\ln\left(\frac{\sqrt{1-\beta^2}}{1+\beta\cos\theta}\right)d\theta\right]\end{aligned} \tag{55}$$

But one can also start directly with products, using two-by-two geometric averages between points symmetrically positioned apart from $\pi/2$ by an angle ξ ranging from 0 to $\pi/2$.

$$\begin{aligned}&\left\langle\frac{T^{\text{mov}}}{T}\left(\frac{\pi}{2}\pm\xi\right)\right\rangle\\ &= \frac{\sqrt{1-\beta^2}}{\sqrt{\left[1+\beta\cos\left(\frac{\pi}{2}-\xi\right)\right]\left[1+\beta\cos\left(\frac{\pi}{2}+\xi\right)\right]}}\\ &= \sqrt{\frac{1-\beta^2}{1-\beta^2\sin^2\xi}}\end{aligned} \tag{56}$$

This half geometric averaging minimizes the inequality between the global geometric mean and the residual arithmetic mean, which is obtained by summing the geometric means of all symmetric ξ,

$$\left\langle\frac{T^{\text{mov}}}{T}\right\rangle < \frac{2}{\pi}\sqrt{1-\beta^2}\int_{\xi=0}^{\frac{\pi}{2}}\frac{d\xi}{\sqrt{1-\beta^2\sin^2\xi}} \tag{57}$$

whose last term is Legendre's complete elliptic integral of the first kind [26]. The right side of Eq.(57) is less than one since the square root of the elliptic integral should be removed to obtain 1.

$$\frac{2}{\pi}\sqrt{1-\beta^2}\int_{\xi=0}^{\frac{\pi}{2}}\frac{d\xi}{1-\beta^2\sin^2\xi} = 1 \tag{58}$$

More precisely,

$$\left\langle\frac{T^{\text{mov}}}{T}\right\rangle < \frac{2}{\pi}K\left(\frac{\beta^2}{\beta^2-1}\right) \sim 1-\frac{\beta^2}{4}-\frac{7\beta^4}{64} \tag{59}$$

Perceived time appears globally contracted, contrary to a time dilation.

$$\left\langle\frac{T^{\text{mov}}}{T}\right\rangle < 1$$

7.3 Mean Galilean Doppler effect

The geometric mean of the Galilean Doppler effects obtained before and after the nearest point is independent of θ and less than 1. Using Eq.(38) and for periods,

$$\left\langle\frac{T^{\text{mov}}}{T}\right\rangle = \left(\prod_{\theta=0}^{\pi}\frac{T_{(\theta)}^{\text{mov}}}{T}\right)^{\frac{1}{\pi}} = \sqrt{1-\beta^2} \sim 1-\frac{\beta^2}{2}-\frac{\beta^4}{8} \tag{60}$$

7.4 Comparison of the mean Galilean and relativistic values

For the Galilean circle, the situation is geometrically clear. On the axis crossing the source and orthogonal to its trajectory, the wavefronts are narrowed by $\sqrt{1-\beta^2}$, narrower in front of this axis and wider behind it, with an overall average equal to the transverse axis. Strikingly,

the properties of this axis are exactly the same for the ellipse (compare the yellow lines between Table 1 and Table 2 in Appendix B). However, since the ellipse is longer at the back, the global average of the distances between successive wave crests is slightly higher.

8 Discussion

Although electromagnetic and Galilean waves are fundamentally different in nature, it is instructive to compare their properties. Their differences in terms of aberration and Doppler effect are more subtle than expected and depend entirely on their respective received wavefronts: ellipsoidal for electromagnetic waves and spherical for Galilean waves. This joint study also suggests some explanations for the maintenance of an erroneous classical Doppler formula in the recent literature and in university courses. In fact, the currently accepted Doppler equation has been strangely shaped by the knowledge of the relativistic one, while the two Doppler effects obey radically different laws. It suffers from unproven assumptions widely used in textbooks such as: (1) there is no transverse classical Doppler effect; (2) the relativistic Doppler effect corresponds to the Galilean Doppler effect modified by the Lorentz dilation factor. Einstein himself took the previous formula of the Doppler effect (not yet called classical) for granted, which logically led him to believe that the transverse effect he had discovered was specific to the relativistic Doppler effect. His contributions were so important that he cannot be asked to verify the previous formulas. The timing of perceived durations, like the Doppler and aberration effects, is a receiving process that depends on the velocity vector. Unlike the time dilation of special relativity, perceived time is not uniform in a global inertial frame. The appropriate tool for converting proper to proper durations is the Doppler effect, which applies not only to wave periods, to which it is usually limited, but to any duration. The Doppler effect is generally considered to be a long-established phenomenon, corresponding to a dead branch of fundamental physics, now confined to general education. According to the historical recollections of [27], one of the difficulties Christian Doppler had in convincing the scientific community in 1842 was that his theory seemed too mathematically simple to describe physics. As this study suggests, using only elementary algebra, the Doppler effect seems to remain both mathematically simple and physically subtle.

Acknowledgements. I thank S. Di Matteo for enlightening discussions.

This research did not receive any specific grant from funding agencies in the public, commercial, or not-for-profit sectors.

References

[1] G. Lemaître, Un Univers homogène de masse constante et de rayon croissant rendant compte de la vitesse radiale des nébuleuses extra-galactiques. Annal. Soc. Sci. Bruxelles A47 (1927) 49-59.

[2] S. Perlmutter, Supernovae, dark energy, and the accelerating universe: The status of the cosmological parameters. Proceedings of the XIX International Symposium on Lepton and Photon Interactions at High Energies. Stanford, California (1999). PDF proceeding

[3] T.W. Hänsch, A.L Schawlow, Cooling of gases by laser radiation. Optics Communications 13 (1975) 68. doi:10.1016/0030-4018(75)90159-5

[4] C. Doppler, Über den Einfluss der Bewegung des Fortpflanzungsmittel auf die Erscheinungen der Äther-, Luft- und Wasserwellen: ein weiterer Beitrag zur allgemeinen Wellenlehre (On the Influence of the motion of the propagating medium on the phenomena of ether, air and water waves: a further contribution to general wave theory), Borrosch (1847)

[5] Y. Pierseaux, Special relativity: Einstein's spherical waves versus Poincare's ellipsoidal waves. Annales de la Fondation Louis de Broglie 30 (2005) 353-379.

[6] A. Einstein, Zur Elektrodynamik bewegter Körper (On the electrodynamics of moving bodies) Annal. Phys. 17 (1905) 891-921. doi:10.1002/andp.19053221004

[7] H. Poincaré, Le principe de Relativité. La dynamique de l'électron. Revue Générale des Sciences Pures et Appliquées 19 (1918) 386-402.

[8] L. Meléndez, On the violation of the Lorentz invariant. Phys. Assays 22 (2009) 489-492.

[9] D. Michel, Galilean and relativistic Doppler/aberration effects deduced from spherical and ellipsoidal wavefronts respectively. Optik 250 (2002) 168242. doi:10.1016/j.ijleo.2021.168242

[10] W. Moreau, Wave front relativity. Am. J. Phys. 62 (1994) 426-429. doi:10.1119/1.17543

[11] H. Boutayeb, Michelson-Morley experiment, general Doppler´ s principle, Maxwell´ s equations, particle accelerators and Mössbauer experiment (2019) preprint

[12] Y.V. Chesnokov, I.V. Kazachkov, Analysis of the Doppler effect based on the full Maxwell equations. Equations 2 (2022) 100-103. doi:10.37394/232021.2022.2.16

[13] G. Joos, I.M. Freeman, Theoretical Physics. Hafner publishing company NY (1913)

[14] S. Klinaku, The Doppler effect is the same for both optics and acoustics. Optik 244 (2021) 167565. doi:10.1016/j.ijleo.2021.167565

[15] A.H. Compton, A quantum theory of the scattering of X-rays by light elements. Phys. Rev. 21 (1923) 483-502. doi:10.1103/PhysRev.21.483

[16] A.D. Pierce, Acoustics: An introduction to its physical principles and applications. 3d Ed. Springer (2019) doi:10.1007/978-3-030-11214-1

[17] O. Alejos, J.M. Muños, A review of the classical Doppler effect based on the mathematical description of the phase function (2023) https://arxiv.org/abs/2308.08566.

[18] D. Sher, The Relativistic Doppler Effect. Journal of the Royal Astronomical Society of Canada 62 (1968) 105-111

[19] T.P. Gill, The Doppler Effect. London, Logos Press Limited (1965).

[20] R.P. Feynman, R.B. Leighton, M. Sands, Relativistic Effects in Radiation. The Feynman Lectures on Physics. Reading, Massachusetts: Addison-Wesley. 1 (1977) 3437.

[21] D. Morin, Introduction to classical mechanics: with problems and solutions. Cambridge University Press. Chapter 11: Relativity (Kinematics) (2008) 539-543.

[22] H.E. Ives, G.R. Stillwell, An experimental study of the rate of a moving atomic clock.J. Opt. Soc. Am. 28 (1938) 215-226. doi:10.1364/josa.28.000215

[23] D. Hasselkamp, E. Mondry, A. Scharmann, Direct observation of the transversal Doppler-shift. Z. Phys. A 289 (1979) 151-155. doi:10.1007/BF01435932

[24] M. Fowler, The Doppler effect.Virginia courses link

[25] A. Einstein, Über die Möglichkeit einer neuen Prüfung des Relativitätsprinzips (On the possibility of a new test of the relativity principle) Annal. Phys. 328 (1907) 197-198. doi:10.1002/andp.19073280613

[26] P.F. Byrd, M.D. Friedman, Handbook of Elliptic Integrals for Engineers and Scientists; Springer: New York, NY, USA (1971). doi:10.1007/978-3-642-65138-0

[27] D.D. Nolte, The fall and rise of the Doppler effect. Phys. Today 73 (2020) 30-35. doi:10.1063/PT.3.4429

[28] R.A. Mangiarotty, B.A. Turner, Wave radiation doppler effect correction for motion of a source, observer and the surrounding medium. J. Sound Vib. 6 (1967) 110-116. doi:10.1016/0022-460X(67)90163-0

Appendices

A Classical Doppler measurement

The relativistic Doppler effects predicted by Einstein have been perfectly verified experimentally in their longitudinal [22] and transverse [23] versions, but curiously the angular Doppler effect, which predates relativity, has remained little studied. Moreover, the study of [23] was based on the unverified idea that the so-called classical Doppler effect has no transverse effect, which is disputed here. Any ordinary movie is a joint recording of image and sound, but since these two types of waves reach the camera and microphone at different speeds, they actually describe separate moments in the recent past (Fig.6). To illustrate this subtlety, let us analyze the shift in sound frequency during the passage of an airplane by analyzing image and sound in parallel.

A.1 Determination of an airplane speed and rest frequency

The asymptotic values of the apparent frequencies heard when the source arrives, written f_a and those measured when the source recedes, written f_r, are sufficient to determine the source velocity, even without knowing the source frequency f_0. Indeed, f_a and f_r are related by

$$f_0 = f_a\,(1-\beta) = f_r\,(1+\beta) \tag{A.1a}$$

from which

$$\beta = \frac{f_a - f_r}{f_a + f_r} \tag{A.1b}$$

The frequencies given by the spectrogram f_a=6750 Hz and f_r=4338 Hz, give $\beta = 0.2175$ (at 15°C, 74 m/s or 266 km/h). Once β is known, the equalities of Eq.(A.1a) allow us to find the rest frequency: $f_0 = 5282$ Hz. Note that although it is called rest frequency, f_0 may not exist when the aircraft is stopped with the engines on, for example if this sound is generated by the flow of the apparent wind.

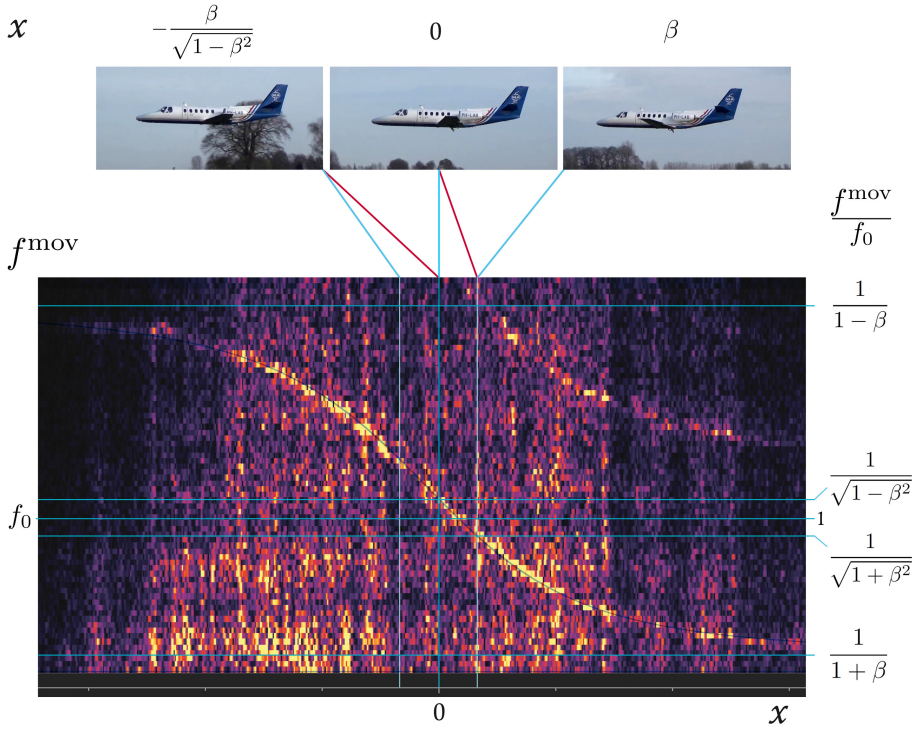

Figure A1. Doppler effect illustrated by a dominant frequency recorded during the passage of an airplane at low altitude. The blue lines connecting the images of the planes to the spectrogram indicate the actual coincidence of sound and image on the film, while the red lines connect the recorded frequencies to their actual points of emission.

A.2 Doppler formulas as a function of distance

Angular Doppler formulas are not very practical for analyzing experimental results because they compress the far zones and induce a distortion between the linear recording of the moving source at constant speed. The correspondence between any angle ϑ and the distance is

$$D = -X \tan\vartheta \tag{A.2}$$

where D is the shortest source-observer distance over the whole source trajectory, and X is the distance of the source from this closest point.

$$\frac{X}{D} = x = -\frac{\cos\vartheta}{\sqrt{1-\cos^2\vartheta}} \tag{A.3}$$

$$\cos\vartheta = -\frac{x}{\sqrt{1+x^2}} \tag{A.4}$$

By applying this relation to the angles θ and θ' presented previously, we obtain, for the classical Doppler formula

$$\left(\frac{f^{\text{mov}}}{f}\right)_{\text{classical}} = \frac{1}{1+\dfrac{\beta x'}{\sqrt{1+x'^2}}} \tag{A.5}$$

and for the formulas deduced from the spherical wavefront, the Doppler effects are described as functions of the coordinates of the position of the source (P) and of the emission point (E), by setting $\vartheta = \theta$ or θ' respectively.

$$\left(\frac{f^{\text{mov}}}{f}\right)_P = \frac{\sqrt{1+x^2}}{\beta x + \sqrt{1-\beta^2+x^2}} \tag{A.6}$$

and

$$\left(\frac{f^{\text{mov}}}{f}\right)_E = \frac{1}{\sqrt{1+\beta^2+2\beta\dfrac{x'}{\sqrt{1+x'^2}}}} \tag{A.7}$$

As a check, we can verify that Eq.(A.6) gives the average Doppler effect determined with its angular counterpart Eq.(60). The geometric mean of the Galilean Doppler effect is

$$\forall x,\ \left\langle \frac{f(-x)}{f_0}, \frac{f(+x)}{f_0} \right\rangle = \frac{1}{\sqrt{1-\beta^2}} \tag{A.8}$$

The Doppler effect of the sound is naturally carried by the acoustic wave but the information about the position of the source is generally visual, i.e. carried by light (Fig.6). When the wave emitted in X reaches the receiver, the source has traveled a distance that depends on the duration Δt of the flight of the wave from the source to the receiver. This path, of length $c\Delta t$, is the hypotenuse of a right triangle whose other two sides are the shortest distance D, and the distance X separating the source from the nearest point. So Pythagoras says

$$(c\Delta t)^2 = D^2 + X^2 \tag{A.9a}$$

from which

$$\Delta t = \frac{\sqrt{D^2+X^2}}{c} = D\frac{\sqrt{1+x^2}}{c} \tag{A.9b}$$

During this time, the source will have traveled

$$\Delta X = v\Delta t = \beta D\sqrt{1+x^2} \tag{A.9c}$$

or in normalized distance

$$\Delta x = \beta\sqrt{1+x^2} \tag{A.9d}$$

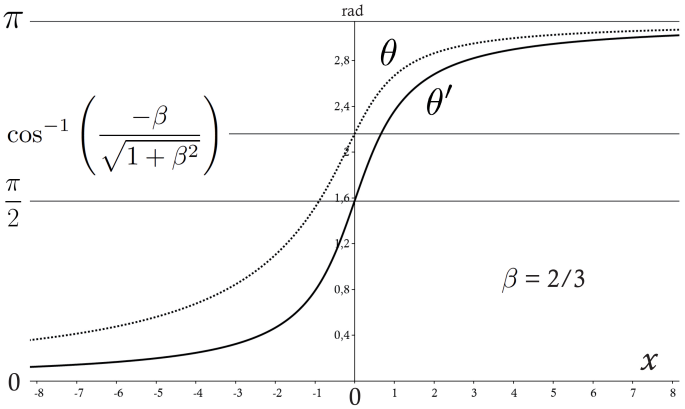

Figure A2. Plots of Galilean angular aberration as a function of distance. Dashed curve: Angle θ between the trajectory of the source and the source-receiver direction according to Eq.(A.10). Solid line curve: angle θ' between the trajectory of the source and the line connecting the emission point to the receiver.

The point of emission can be calculated from the actual position of the source when the Doppler effect is detected. The angle $\theta' = \cos^{-1}\left(-\dfrac{x}{\sqrt{1+x^2}}\right)$ whose origin is the point of emission, is expected to become θ when replacing x by $x + \Delta x$,

$$\theta = \cos^{-1}\left(\frac{-(x+\beta\sqrt{1+x^2})}{\sqrt{1+(x+\beta\sqrt{1+x^2})^2}}\right)$$

which can be rewritten

$$= \cos^{-1}\left(\frac{\left(-\dfrac{x}{\sqrt{1+x^2}}\right)-\beta}{\sqrt{1+\beta^2-2\beta\left(-\dfrac{x}{\sqrt{1+x^2}}\right)}}\right) \tag{A.10}$$

Expectedly in this form, Eq.(A.10) is analogous to the aberration formula Eq.(37c). These functions are shown in Fig.A2. The introduction of Eq.(A.10) into the Doppler formula Eq.(38), gives back the curve of Eq.(A.7). Conversely, the introduction into the Doppler formula Eq.(39) of the angle θ obtained by conversion of $\cos^{-1}\left(-\dfrac{x}{\sqrt{1+x^2}}\right)$ by the aberration formula Eq.(37b), gives the curve of Eq.(A.6). The Doppler functions derived from this approach are shown in Fig.A3.

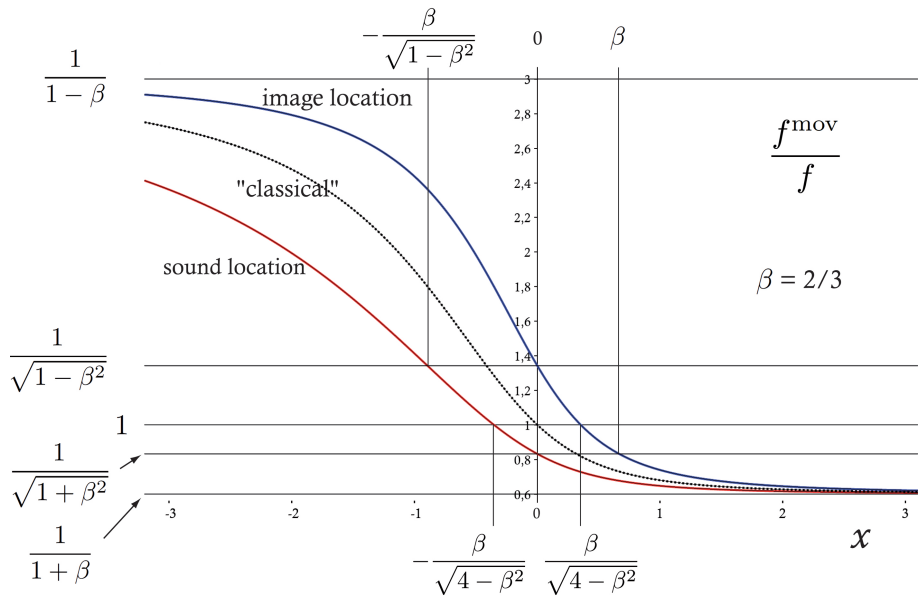

Figure A3. Doppler effect of the sound as a function of the relative position of a moving source on its path, for a stationary receiver in the absence of wind, expressed as a function of either the coordinate of the emitting point (lower red curve drawn to Eq.(A.7)), or of the visually detected source (upper blue curve drawn to Eq.(A.6)). The dashed black curve shown for comparison is that of the classical Doppler formula drawn to Eq.(A.5). The increment of the coordinate x is the minimum distance between the source and the receiver.

A.3 Curve fitting and conclusions

The theoretical equation combining the simultaneously recorded image and sound is Eq.(A.6) where the ordinate is the sound Doppler shift and the abscissa x is the spatial coordinate of the source determined visually. Inserting the previously measured value of β into this equation gives the horizontal increment $x = 1$. At $x = 0$ (5156 Hz, Doppler effect of 1.025) the observer's line of sight is perpendicular to the plane trajectory. The Doppler effect for $x = 0$ is expected to be

$$\left.\frac{f^{\mathrm{mov}}}{f_0}\right|_{\mathrm{orthogonal}} = \frac{1}{\sqrt{1-\beta^2}}$$

As explained in the main text, this is not the transverse Doppler effect which is

$$\left.\frac{f^{\mathrm{mov}}}{f_0}\right|_{\mathrm{transverse}} = \frac{1}{\sqrt{1+\beta^2}}$$

This latter effect (5156 Hz, Doppler effect of 0.977) is received only when the plane has moved away from the transverse position by a distance βD from the nearest point. Given the delay of 0.323 seconds measured from the video, it corresponds to 110 m from the transverse position. In summary, the accuracy of the curve fit shown in Fig.A3 can be verified by checking the frequencies for the following two points:

- $x = 0 \rightarrow f^{\mathrm{mov}} = f_0/\sqrt{1-\beta^2}$
- $x = \beta \rightarrow f^{\mathrm{mov}} = f_0/\sqrt{1+\beta^2}$

In addition, for image and sound to match, $x = 0$ must coincide with the most transverse position of the source. This can be seen in Fig.A1 in the apparent orientation of the wings and the alignment of the side windows of the cockpit. Once these three criteria are met, the rest of the curve fits remarkably well (Fig.A1). The blue lines connect the images and the sounds which are superimposed on the video. But this apparent simultaneity is only an illusion of reception, as shown by the red lines that connect the sound to the position of the plane where it was actually emitted. This offset is, of course, due to the difference in speed between light and sound to get from the plane to the camera [28]. The sound received when the plane is seen perfectly in profile was sent at the position $x = -\beta/\sqrt{1+\beta^2}$, which would belong to the curve drawn to Eq.(A.7) if added to the same diagram.

B Points of comparison between relativistic and Galilean angular Doppler effects

Table 1: Some relativistic correspondences between angles, distances and Doppler effects. The line highlighted in green corresponds to the transverse Doppler effect and that highlighted in yellow color is the only common point with the Galilean Doppler effect of Table 2.

Origin of the angle		Distance to the nearest point of the		Doppler effect
source	point of emission	source position	sound emission	
θ	θ'	x	x'	f^{mov}/f
0	0	$-\infty$	$-\infty$	$\sqrt{\frac{1+\beta}{1-\beta}}$
$\frac{\pi}{2}$	$\cos^{-1}\beta$	0	$-\frac{\beta}{\sqrt{1-\beta^2}}$	$\frac{1}{\sqrt{1-\beta^2}}$
$\cos^{-1}-\frac{1-\sqrt{1-\beta^2}}{\beta}$	$\cos^{-1}\frac{1-\sqrt{1-\beta^2}}{\beta}$	$\frac{1}{\sqrt{2}}\sqrt{\frac{1}{\sqrt{1-\beta^2}}-1}$	$-\frac{1}{\sqrt{2}}\sqrt{\frac{1}{\sqrt{1-\beta^2}}-1}$	1
$\cos^{-1}-\beta$	$\frac{\pi}{2}$	$\frac{\beta}{\sqrt{1-\beta^2}}$	0	$\sqrt{1-\beta^2}$
π	π	$+\infty$	$+\infty$	$\sqrt{\frac{1-\beta}{1+\beta}}$

Table 2: Some Galilean correspondences between angles, relative distances and Doppler effects. The unit of angle is radian and the unit of distance is the minimum distance between the mobile source and the stationary receiver. The line highlighted in green corresponds to the transverse Doppler effect and that highlighted in yellow color is the only common point with the relativistic Doppler effect (Table 1).

Origin of the angle		Distance to the nearest point of the		Doppler effect
source	point of emission	source position	sound emission	
θ	θ'	x	x'	f^{mov}/f
0	0	$-\infty$	$-\infty$	$\frac{1}{1-\beta}$
$\frac{\pi}{2}$	$\cos^{-1}\beta$	0	$-\frac{\beta}{\sqrt{1-\beta^2}}$	$\frac{1}{\sqrt{1-\beta^2}}$
$\cos^{-1}-\frac{\beta}{2}$	$\cos^{-1}\frac{\beta}{2}$	$\frac{\beta}{\sqrt{4-\beta^2}}$	$-\frac{\beta}{\sqrt{4-\beta^2}}$	1
$\cos^{-1}-\frac{\beta}{\sqrt{1+\beta^2}}$	$\frac{\pi}{2}$	β	0	$\frac{1}{\sqrt{1+\beta^2}}$
π	π	$+\infty$	$+\infty$	$\frac{1}{1+\beta}$